Bentonite-Carbide Slag Composite for AMD Treatment

Kutlwano Tshwaedi and Elvis Fosso-Kankeu

***Abstract*—** This study investigates the efficacy of a bentonite-calcium carbonate composite for treating acid mine drainage (AMD) with the aim of reducing metal ion concentrations and neutralizing acidity. AMD samples exhibited a highly acidic pH of 1.881 and high oxidation-reduction potential (ORP) of 665.8 mV, which facilitated the solubilization of metal ions. Atomic Absorption Spectroscopy (AAS) identified high levels of iron (Fe), calcium (Ca), and magnesium (Mg) as the dominant metal ions, with lower concentrations of nickel (Ni), copper (Cu), chromium (Cr), and potassium (K). Experiments were conducted in 150 mL solutions using both activated and unactivated forms of the composite, with adsorption efficiency evaluated through kinetic models. Results showed that adsorption increased with time and was best described by the pseudo-second-order kinetic model, especially for the activated composite, indicating a chemisorption mechanism. The activated composite achieved higher adsorption capacities and removal efficiencies, particularly at lower sample masses, likely due to enhanced surface properties from calcination. The adsorption capacity was inversely related to composite mass, with 0.1 g samples displaying the highest values. Additionally, the composite effectively increased the pH of the solution, providing a buffering effect that could mitigate AMD's extreme acidity. The combination of high adsorption efficiency and pH neutralization suggests that the bentonite-calcium carbonate composite is a promising material for AMD treatment. These findings support its potential use for mitigating the environmental impact of metal-contaminated and acidic mine waters, with implications for future remediation strategies.

***Keywords*—** AMD, Bentonite Carbide Slag Composite, Metals, Ph, Mining.

I. Introduction

Acid mine drainage is a significant environmental concern in South Africa, particularly in the coal mining regions of Mpumalanga. The oxidative weathering of pyrite and other sulphide minerals in mine tailing and waste rock leads to the generation of acid mine drainage, which is characterized by its low pH, strong acidity, and high concentrations of heavy metals such as manganese (Mn), Aluminium (Al), Lead (Pb), Chromium (Cr) , Cadmium (Cd) ,Cobalt (Co) and Nickel (Ni) [1-4]. Acid mine drainage has caused serious damage to environmental and socio-economic harm, including water and soil pollution, health risks, environmental degradation, economic impacts, infrastructure damages, loss of biodiversity and negative impacts on agriculture [5]. Acid mine drainage has been mitigated through various treatments. These treatments include chemical, biological, passive, active, in situ, ex situ , natural attenuation, phytoremediation and permeable reactive barriers. In the recent years, research has focused on developing sustainable and effective passive treatment technologies such as composite materials to neutralize and remove heavy metals acid mine drainage [6]. This project investigates the potential of a composite material consisting of bentonite clay and carbide slag. Bentonite is naturally occurring clay mineral and its main component is montmorillonite, a type of smectite clay and has been proven to be effective in adsorbing heavy metals. Carbide slag is a by-product of steel industries and its produced in the industry production of acetylene gas, and its main component is $Ca(OH)_2$ [7], it contains alkaline properties that can neutralize acidity in the acid mine drainage. Numerous research results have shown that alkaline composite particle adsorbents continuously release alkalinity during acid mine drainage treatment and have a synergistic effect of neutralization adsorption coagulation on H^+ and heavy metal ions. Previous publication has shown that bentonite clay can be combined with carbide slag to obtain a bentonite carbide-slag composite particle that exhibits good performance for mitigation of acid mine drainage [8].

A. Research problem statement

Acid mine drainage has become a major environmental issue, causing serious damage to ecosystems and the health of communities. It has been linked to the loss of biodiversity, decreased crop yield, and increased incidence of respiratory and digestive diseases in humans. In addition, acid mine drainage is a major source of pollution to rivers and lakes, contaminating drinking water supplies and affecting aquatic life. If left unchecked, Acid mine drainage will continue to cause significant damage to the environment and human health, with potentially devastating consequences. Therefore, it is important that a solution is found.

The aim of this study is to investigate the efficiency of bentonite-carbide slag on the treatment of acid mine drainage.

Kutlwano Tshwaedi[1], Department of Metallurgy at the University of Johannesburg in South Africa.

Elvis Fosso-Kankeu[2], Department of Metallurgy at the University of Johannesburg in South Africa

https://doi.org/10.17758/IICBE6.C1124144

II. METHODOLOGY

A. Characterization of the composite and the AMD solution

The calcium carbonate and the bentonite will mixed and characterized to determine their properties before calcining using XRF, SEM ,BET and FTIR analysis. The calcined calcium carbonate-bentonite will then be characterized to understand its properties when calcined carbonate and bentonite are combined as a composite using XRF, SEM,BET and FTIR analysis. The AMD will be diluted using deionized water reduce its concentration. Temperature, pH and ORP will be tested from the AMD using multiparameter tester. The AMD will then be characterized using AAS to determine the metal ions concentration.

B. Preparation of the calcined BCS composite

A mixture of 100g of calcium carbonate with 100g of bentonite and 4g of sodium carbonate which acts as a binder was mixed to ensure even distribution of the binder. The mixture was calcined in a graphite crucible at 850˚C for 1hour.The mixture was cooled down for 1 hour. Samples for XRF, SEM ,BET and FTIR analysis will then be from prepared from the calcined samples.

C. Adsorption experiments

A sample of 600mL of AMD was prepared by diluting 60mL of AMD by 540mL of deionized water. A sample of 300mL diluted AMD was taken and divided into 2 beakers for calcined composite and inactivated composite experiments. The mass dosage and the adsorption time was varied simultaneously with mass dosages of 0.1g, 0.2g, and 0.3g of the calcined calcium bentonite and the inactivated calcium carbonate bentonite composite on different beakers. The time varied in units 0f 10 minutes up until 50 minutes. The experiments were run at 35˚C at 250rpm. The beaker with the diluted AMD was put on top of the magnetic stirrer and the composite mass of 0.1 was added into the solution every 10 minutes a sample was taken. After each experiments filter papers was used to separate solid from liquid.2mL of diluted nitric acid will be added to each sample for preservation. Samples will then be stored and labelled in 40mL test tubes before AAS analysis.

III. RESULTS AND DISCUSSION

A. Figures and Tables

TABLE I: XRF ANALYSIS OF THE CALCINED BENTONITE CALCIUM CARBONATE COMPOSITE

Component	Result	convertion	Elemental	%mass
Na2O	1.8463	0.71486	Na	1.31984602
MgO	1.9997	0.6031	Mg	1.20601907
Al2O3	8.1586	0.52925	Al	4.31793905
SiO2	23.1194	0.46744	Si	10.8069323
P2O5	0.0453	0.43642	P	0.01976983
SO3	0.2308	0.40049	S	0.09243309
Cl	0.0406		CI	0.0406
K2O	0.5851	0.83016	K	0.48572662
CaO	54.1583	0.7147	Ca	38.706937
TiO2	0.5924	0.59951	TI	0.35514972
MnO	0.0853	0.77446	Mn	0.06606144
Fe2O3	9.0921	0.69943	Fe	6.3592875
ZnO	0.011	0.80337	Zn	0.00883707
SrO	0.0192	0.84559	Sr	0.01623533
ZrO2	0.0159	0.74031	Zr	0.01177093
			total	63.813545
			O2	36.186455

In the XRF analysis of both activated and unactivated composites, notable elemental concentrations were observed in calcium (Ca), iron (Fe), and silicon (Si). The data reveal a pronounced presence of these elements in both states, underscoring their substantial roles in the composite matrix. Specifically, the activated composite, which was subjected to a calcination process, exhibited a slight increase in calcium content compared to its unactivated counterpart. The increase in calcium in the activated composite can be attributed to the effects of thermal treatment during calcination. Calcination often leads to changes in mineral phases, potentially enhancing the detectability or concentration of certain elements due to alterations in the crystalline structure or release of volatile components that might otherwise obscure calcium signals. Additionally, the thermal activation may have facilitated the breakdown of less stable compounds, thereby concentrating more stable calcium-bearing phases. Overall, the results indicate that while calcination primarily impacts calcium content, it does not significantly alter the iron or silicon composition. This stability in Fe and Si concentrations may be advantageous in applications where thermal treatment is required without affecting these elemental constituents. The slight increase in calcium in the activated composite may enhance certain adsorption properties, potentially impacting reactivity, durability, or other performance factors.

https://doi.org/10.17758/IICBE6.C1124144

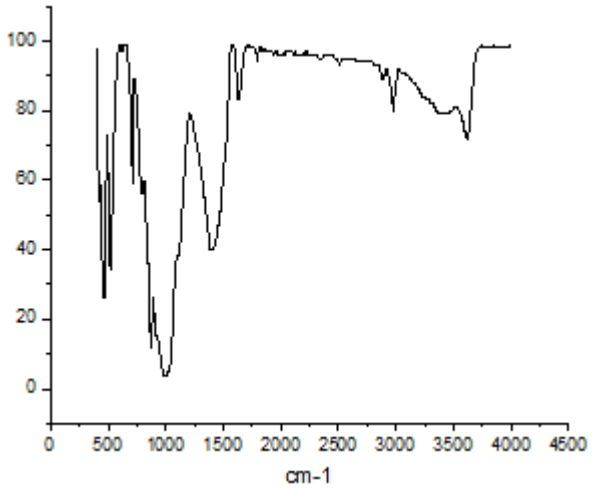

Fig. 1: FTIR Analysis of inactivated composite

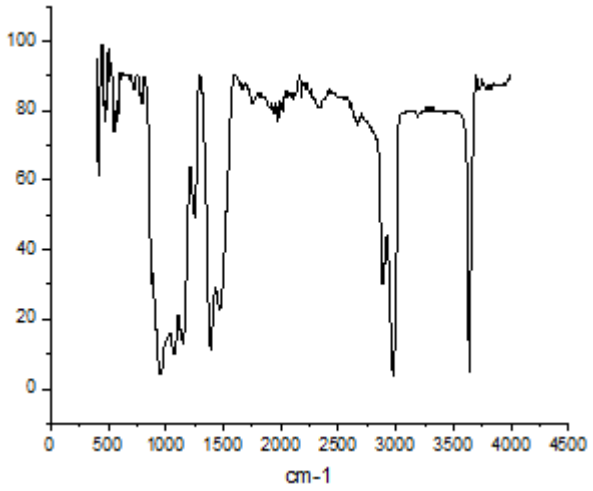

Fig. 1: FTIR Analysis of activated composite

The FTIR analysis of the unactivated and activated composites reveals distinct differences in the vibrational spectra, particularly in the number and intensity of absorption peaks. The infrared (IR) spectrum of raw and activated composite revealed several significant peaks including, peaks at 712 cm^{-1}, 872 – 873 cm^{-1} and 1420 cm^{-1} or 1400 cm^{-1} indicating the presence of O-C-O group from CO3, as well as asymmetric stretching mode for C-O. Other peaks at 3000 and 2899.9 cm^{-1} were attributed to stretching vibrations of O-H from water, suggesting the existence of hydration.

The unactivated composite exhibited fewer peaks, suggesting a simpler and potentially less reactive surface profile compared to the activated composite. This reduced peak count indicates that fewer functional groups are present on the surface of the unactivated composite, potentially due to limited accessibility of active sites or reduced structural complexity prior to activation.

In contrast, activated composite showed a greater number of absorption peaks, which signifies an increase in available functional groups and surface-active sites following the thermal treatment. Calcination likely induced structural rearrangements, facilitated the removal of volatile impurities, and exposed previously inaccessible binding sites. The introduction of additional peaks in the FTIR spectrum corresponds to the emergence of new bonds and functional groups that were either created or made more detectable post-calcination.The increase in spectral peaks in the activated composite is crucial for adsorption applications, as it suggests enhanced interaction sites for adsorbates. These additional functional groups—potentially including hydroxyl, carbonyl, and silicate groups—can improve binding affinity and adsorption capacity by providing a more complex surface chemistry and an increase in active adsorption sites. Therefore, the FTIR results imply that calcination not only modifies the surface chemistry but also enhances the potential adsorptive functionality of the composite.

B. Metals removal from AMD

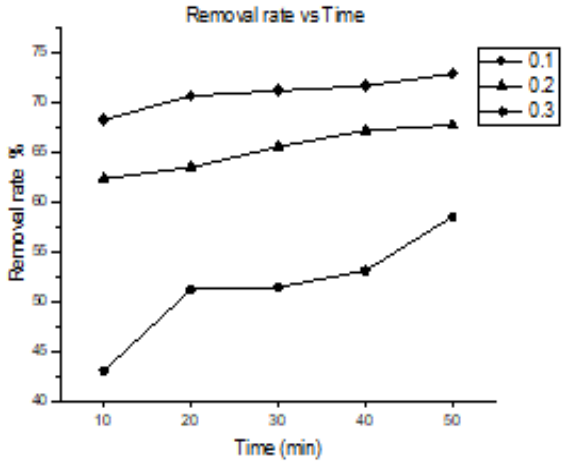

Fig. 2: Fe removal rate using inactivated composite

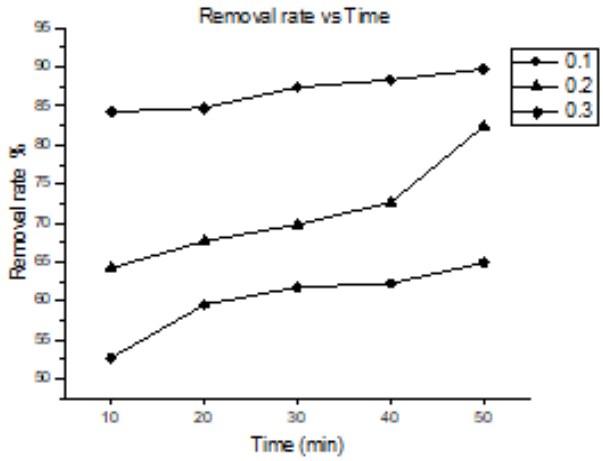

Fig. 3: Fe removal rate using activated composite

The adsorption experiments conducted to assess the Fe removal rate over time for both activated and unactivated composites reveal significant variations in efficiency based on sample mass and treatment conditions. The results indicate that both the amount of composite added and the activation state of the composite substantially impact the removal

https://doi.org/10.17758/IICBE6.C1124144

performance. This relationship is explored by analyzing the Fe removal rates at different sample masses (0.1g, 0.2g, and 0.3g) and across time intervals ranging from 10 to 50 minutes. For the unactivated composite, the Fe removal rate showed a gradual increase over time, reaching maximum values at 50 minutes across the different sample masses. At a lower mass of 0.1g, the removal rate achieved at 50 minutes was 58%, which represents a moderate level of Fe adsorption. As the sample mass increased to 0.2g, a higher removal rate of 65% was observed, indicating that increasing the adsorbent quantity can enhance the adsorption capacity. With 0.3g of the unactivated composite, the removal rate at 50 minutes further increased to 73%, demonstrating that additional mass leads to more adsorption sites, thereby enhancing Fe removal.

These findings suggest that for the unactivated composite, while Fe removal efficiency does improve with increased adsorbent mass, the rate remains lower than that achieved by the activated composite. This may be due to the limited surface area and fewer active functional groups on the unactivated composite, as confirmed by the FTIR analysis. The activated composite exhibited superior Fe removal rates across all sample masses and at each time point compared to the unactivated counterpart. With a 0.1g sample mass, the Fe removal rate reached 62% at 50 minutes, already surpassing the highest performance of the unactivated composite under similar conditions. At 0.2g, the activated composite achieved an Fe removal rate of 81% at 50 minutes, and at 0.3g, the removal rate further increased to 89%. These results indicate that the calcination process enhanced the adsorptive capabilities of the composite, likely by increasing the availability of active sites and functional groups, as noted in the FTIR analysis. The trend observed with the activated composite, in which the Fe removal rate improves significantly with increased sample mass, suggests that the activated composite's surface is more conducive to Fe binding. This enhanced performance can be attributed to the structural and chemical modifications induced by activation, which likely exposed additional adsorption sites and increased the composite's surface area. Across both activated and unactivated composites, the removal rate of Fe consistently increased with time, demonstrating that prolonged exposure allows for greater Fe ion uptake. At each time interval, the activated composite consistently outperformed the unactivated composite, indicating that the calcination process accelerated the adsorption rate.

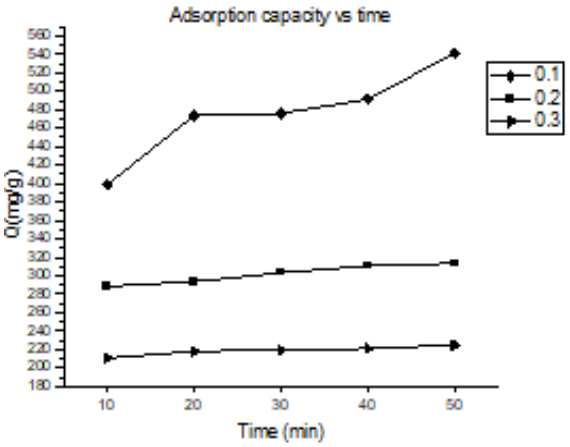

Fig. 4: Adsorption capacity of Fe on inactivated composite

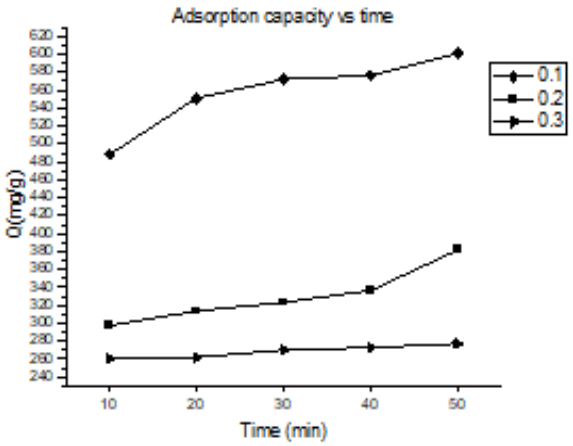

Fig 5: Adsorption capacity of Fe on activated composite

The adsorption experiments, focusing on adsorption capacity versus time, reveal a distinctive relationship between composite mass and adsorption capacity. The results show that adsorption capacity decreases as the composite mass increases, and that activated composites exhibit higher adsorption capacities than unactivated composites across all time intervals and sample masses. In the unactivated composite, the adsorption capacity is inversely related to the sample mass. With a 0.1g sample, the unactivated composite demonstrated the highest adsorption capacity across the time intervals, suggesting that, per unit mass, fewer adsorption sites are saturated and more Fe ions are adsorbed on the surface. As the mass increased to 0.2g and 0.3g, the adsorption capacity decreased, indicating a decline in Fe ion uptake per unit mass. This decrease may stem from overlapping or competitive adsorption sites within the unactivated composite structure, leading to reduced adsorption efficiency at higher masses. The activated composite displayed higher adsorption capacities at each mass level compared to the unactivated composite, illustrating the enhancement in adsorption efficiency due to thermal activation. At 0.1g, the activated composite achieved the highest adsorption capacity among all tested samples, significantly surpassing the unactivated composite's capacity. Similar to the unactivated composite, the adsorption capacity

https://doi.org/10.17758/IICBE6.C1124144

of the activated composite decreased with increased mass (from 0.1g to 0.3g). However, despite this decrease, the activated composite consistently maintained higher adsorption capacities, suggesting that calcination enhanced the accessibility and availability of adsorption sites on the composite's surface.

Kinetics studies

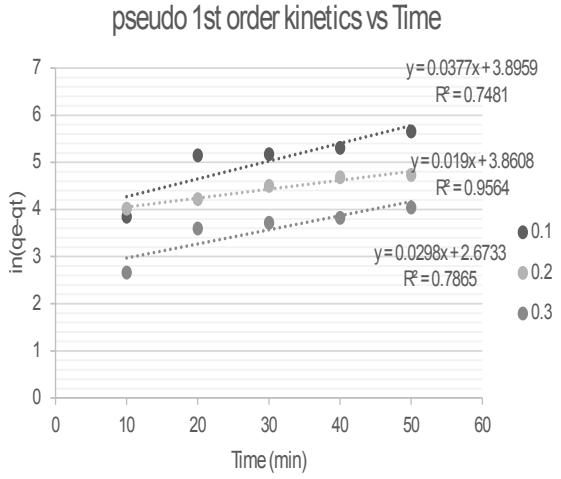

Fig. 6: Pseudo 1st order kinetics on inactivated composite

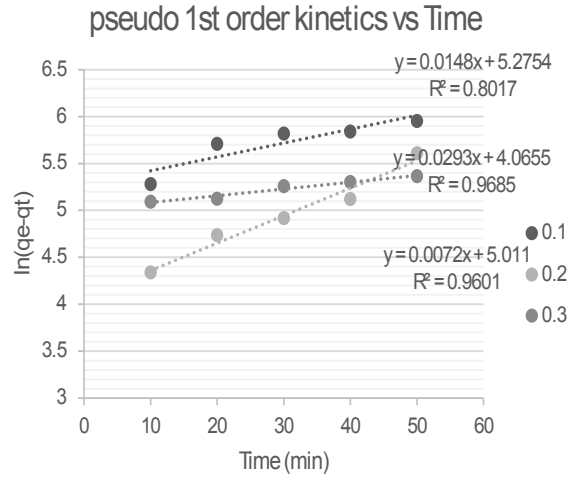

Fig 7: Pseudo 1st order kinetics on activated composite

In evaluating the adsorption kinetics of Fe ions onto the composite materials, the pseudo-first-order kinetic model was applied to determine the adsorption rate and mechanism, as well as to compare the coefficients of determination (R^2 values) across different composite masses and activation states. The R^2 values provide insight into how well the pseudo-first-order model fits the experimental data, indicating whether the adsorption process may be primarily governed by the adsorbate concentration and the availability of surface sites. For the unactivated composite, the coefficients of determination (R^2) varied across the sample masses, suggesting differences in how closely the adsorption process followed the pseudo-first-order model. At 0.2g, the unactivated composite exhibited the highest correlation of 0.9564, indicating a strong fit to the pseudo-first-order kinetic model. This suggests that at 0.2g, the adsorption process for Fe ions on the unactivated composite was likely dominated by surface interactions, where the rate depended on the number of available adsorption sites proportional to the Fe ion concentration. However, at lower (0.1g) and higher (0.3g) masses, the correlation coefficients were lower, with values of 0.7481 and 0.7865, respectively. These lower R^2 values indicate a weaker fit to the pseudo-first-order model, implying that the adsorption mechanism may involve additional kinetic influences beyond the model's assumptions. At 0.1g, limited adsorbent mass might lead to rapid saturation of active sites, thus deviating from a purely concentration-driven adsorption process. Conversely, at 0.3g, increased mass might cause inter-particle interactions or reduced accessibility to adsorption sites, leading to deviations from the pseudo-first-order kinetics. The activated composite demonstrated higher correlation coefficients with the pseudo-first-order model across all masses, highlighting a closer adherence to this kinetic behavior after calcination. At 0.2g, the activated composite achieved the highest coefficient of determination of 0.9865, indicating an almost perfect fit to the pseudo-first-order model. This strong correlation suggests that the calcination process enhanced the material's surface properties, making the adsorption of Fe ions more reliant on initial concentration and available adsorption sites and physical interactions/physisoption, consistent with pseudo-first-order assumptions. At other masses, the activated composite continued to show high correlation coefficients, with 0.8017 at 0.1g and 0.9601 at 0.3g. While the correlation is somewhat reduced at 0.1g, the values still exceed those of the unactivated composite, suggesting that calcination improved the surface reactivity and consistency in kinetic behavior. The 0.3g sample's high correlation of 0.9601 with the pseudo-first-order model further reinforces the positive impact of activation on the material's kinetic consistency, likely due to increased surface area and enhanced availability of adsorption sites.

In analyzing the adsorption kinetics for Fe ions on both activated and unactivated composites, the pseudo-second-order kinetic model was applied to evaluate how well it describes the adsorption process. The coefficients of determination (R^2 values) derived from the model provide insight into the kinetics and suggest whether adsorption is potentially governed by chemisorption, involving electron

sharing or exchange between the adsorbent and adsorbate. For the unactivated composite, the pseudo-second-order model yielded high coefficients of determination across all sample masses, with the highest R^2 value of 0.9987 at 0.2g, closely followed by 0.9986 at 0.1g and 0.9889 at 0.3g. These high R^2 values indicate an excellent fit to the pseudo-second-order model, suggesting that the adsorption of Fe ions on the unactivated composite likely involves chemisorption, where the rate of adsorption depends on the square of the number of unoccupied sites. The slightly lower coefficient of determination at 0.3g (0.9889) suggests some deviation from pure pseudo-second-order behavior at this higher mass, possibly due to limited accessibility of adsorption sites within the composite at increased mass. This minor deviation might be attributed to inter-particle effects or restricted diffusion at higher adsorbent loading, which could hinder the adsorption process. Overall, the strong fit to the pseudo-second-order model across masses suggests that the unactivated composite primarily follows a chemisorption mechanism. In the case of the activated composite, the pseudo-second-order model also provided high coefficients of determination, although the trend differs slightly compared to the unactivated composite. The highest correlation was observed at a lower mass of 0.1g (R^2 = 0.9972), indicating that at this mass, the adsorption process is likely governed by chemisorption, with strong adherence to the pseudo-second-order model assumptions. This correlation suggests that, at lower masses, the surface area and active sites of the activated composite are effectively utilized, facilitating a chemisorption-dominated process.

As the mass increased, the R^2 values decreased slightly, with 0.3g yielding a value of 0.985 and 0.2g showing the lowest correlation at 0.8939. This decreasing trend in correlation suggests that, for the activated composite, the pseudo-second-order model fits less well at higher masses, potentially due to factors such as surface site saturation or aggregation effects that limit available surface area. These findings imply that at higher masses, the adsorption process in the activated composite may not exclusively follow a chemisorption mechanism, with potential contributions from other kinetic factors like internal diffusion or site availability.

C. Kinetics models comparison

Based on the provided data, a comparison between the pseudo-first-order and pseudo-second-order kinetic models for Fe ion adsorption onto the activated and unactivated composites reveals distinct differences in model fit, suggesting which model may better describe the adsorption mechanism. For the unactivated composite, the pseudo-second-order model consistently produced higher coefficients of determination across all sample masses. The R^2 values for the pseudo-second-order model were exceptionally high, with 0.9987 at 0.2g, 0.9986 at 0.1g, and 0.9889 at 0.3g. These values indicate an excellent fit, implying that the adsorption process is likely governed by chemisorption, with adsorption rates proportional to the square of unoccupied sites and reflecting interactions beyond simple mass-transfer limitations. In contrast, the pseudo-first-order model yielded lower R^2 values, particularly at 0.1g (0.7481) and 0.3g (0.7865), with a higher correlation of 0.9564 at 0.2g. Although the fit at 0.2g for the pseudo-first-order model was relatively high, it was still lower than the pseudo-second-order model's fit at the same mass. This suggests that while the pseudo-first-order model may offer some insights at certain masses, it does not consistently capture the kinetic behavior as accurately as the pseudo-second-order model for the unactivated composite. For the activated composite, the pseudo-second-order model also provided a stronger fit at lower and higher masses, with R^2 values of 0.9972 at 0.1g and 0.985 at 0.3g. However, at 0.2g, the R^2 for the pseudo-second-order model was only 0.8939, indicating a less ideal fit at this intermediate mass. Nevertheless, the correlation for the pseudo-second-order model was still high enough to suggest a reasonable approximation of the adsorption kinetics. In comparison, the pseudo-first-order model had higher R^2 values only at the 0.2g mass for the activated composite, where it reached 0.9865. However, at 0.1g and 0.3g, the pseudo-first-order model yielded lower R^2 values of 0.8017 and 0.9601, respectively. Although these values suggest a moderate fit, they are consistently lower than those of the pseudo-second-order model at 0.1g and 0.3g.

Given the data, the pseudo-second-order kinetic model consistently offers a better fit for both the unactivated and activated composites across most masses, particularly at 0.1g and 0.3g. The higher R^2 values indicate that the pseudo-second-order model more accurately describes the adsorption kinetics for Fe ions in both composites, likely due to the chemisorption nature of the adsorption process, where electron-sharing or chemical bonding plays a significant role.

IV. CONCLUSION

The aim of this study was to investigate the effectiveness of a bentonite-calcium carbonate composite in treating acid mine drainage (AMD) through adsorption and pH-neutralization experiments. Acid mine drainage, with its highly acidic pH of 1.881 and oxidative environment (ORP 665.8 mV), was characterized by high levels of iron, calcium, and magnesium, with lower concentrations of nickel, copper, chromium, and potassium. These conditions highlight the need for effective treatment to mitigate the mobility and environmental impact of metal ions in AMD. The experiments demonstrated that the bentonite-calcium carbonate composite effectively increased the removal rate of metal ions, with pseudo-second-order kinetics providing the best fit for both unactivated and activated forms, indicating a chemisorption-dominated process. The activated composite showed higher adsorption capacities and removal efficiencies, particularly at lower masses and shorter times, suggesting that calcination improved the material's surface characteristics. Additionally, the pH increased with composite addition, indicating a buffering effect that can counteract AMD's extreme acidity. This pH adjustment, along with efficient metal ion adsorption,

suggests that bentonite-calcium carbonate composites are a promising solution for AMD treatment, capable of reducing both metal ion concentrations and acidity in contaminated waters. Future work may optimize composite mass and activation conditions for enhanced performance.

ACKNOWLEDGMENT

The authors are grateful for the financial support received from the Faculty of Engineering and the Built Environment from the University of Johannesburg in South Africa.

REFERENCES

[1] Elvis Fosso-Kankeu, Alusani Manyatshe, Frans Waanders. 2017. Mobility potential of metals in acid mine drainage occurring in the Highveld area of Mpumalanga Province in South Africa: Implication of sediments and efflorescent crusts. International Biodeterioration and Biodegradation. 119: 661-670. https://doi.org/10.1016/j.ibiod.2016.09.018

[2] Vhahangwele Masindi, Elvis Fosso-Kankeu, Ednah Mamakoa, Thabo T.I. Nkambule, Bhekie B. Mamba, Mu. Naushad , Sadanand Pandey. 2022. Emerging remediation potentiality of struvite developed from municipal wastewater for the treatment of acid mine drainage. Environmental Research. 210: 112944. doi.org/10.1016/j.envres.2022.112944. https://doi.org/10.1016/j.envres.2022.112944

[3] Sadanand Pandey, Elvis Fosso-Kankeu, Johannes Redelinghuys, Joonwoo Kim, Misook Kang. 2021. Implication of biofilms in the sustainability of acid mine drainage and metals dispersion near coal tailings. Science of The Total Environment. 788: 147851. https://doi.org/10.1016/j.scitotenv.2021.147851.

[4] E Fosso-Kankeu. 2018. Synthesized af-PFCl and GG-g-P(AN)/TEOS hydrogel composite used in hybridized technique applied for AMD treatment. Journal of Physics and Chemistry of the Earth. 105: 170-176. https://doi.org/10.1016/j.pce.2018.02.015

[5] Sheibach, RB, Williams, RE, & Genes, BR. (1982). Controlling acid mine drainage from the Ficher Mining District, Oklahoma, United States. International Mine Water, 45–52. Available from: https://doi.org/10.1007/BF02504607

[6] Kefeni, KK, Msagati, TAM. & Mamba, BB. (2017). Acid mine drainage: Prevention, treatment options, and resource recovery: A review. 151, 475–493. Available from: https://doi.org/10/1016/j.jclepro.2017.03.082

[7] Punia, A. (2020). Role of temperature, wind, and precipitation in heavy metal contamination at copper mines: A review. 28, 4056–4072. Available from: https://doi.org/10.1007/s11356-020-11580-8

[8] Bai J, Zhang, H, Xiao,L. (2021). Formation mechanism of carbide slag composite sustained-alkalinity-release particles for the source control of acid mine drainage, Sci. Rep-UK. 20-23. Available from : https://doi.org/10.1038/s41598-021-03277-w.